CCA-592

541.64

Conference Paper

Crystalline Amorphous Interfaces in Polymer Crystals

A. Peterlin

Camille Dreyfus Laboratory, Research Triangle Institute, Research Triangle Park North Carolina, 27709, U. S. A.

Crystalline polymer solids are never ideally crystallized. From the density defect one may formally derive a finite crystalline and amorphous component. The study of polyethylene single crystals by different methods suggests a spatial separation of the components: a crystalline core and two *quasi* amorphous surface layers containing the chain folds. At the interface the amorphous loops are fixed in the crystal lattice. The space requirement of the amorphous conformations can be only met by the assumption of varying loop length. This immediately increases the entropy content of the loops and partly compensates for the reduction caused by the loop ends fixed at the interface and by the limitation of space accessible to the loops by the existence of the crystal lattice. The high energy requirement of the shortest loops with an excess of *gauche* conformations favors large loops and hence increases the thickness of the surface layer. The values obtained for strictly adjacent reentry of all loops are still below the experimental data. A perfect fit seems possible if one assumes that there are a few loops with nonadjacent reentry and some chains with one end free. The former are a consequence of crystallization kinetics and the latter result from the finite number of extremely long loops surpassing the length of single molecules but also from the chain ends of all molecules of the sample because there is a clear tendency of their concentration on the surface of the crystal.

INTRODUCTION

A peculiar property of crystalline polymer solids is the incomplete crystallinity. From density, heat content, heat of fusion, wide angle x-ray scattering, wide line nuclear magnetic resonance, and infrared absorption one deduces that only a finite volume fraction α is crystalline, the rest $(1 - \alpha)$, however, is amorphous. The macromolecules which as a rule are about hundred times longer than the dimensions of the crystals are only partly included in the crystalline lattice and partly in the amorphous matrix. The old fringed micelle concept assuming every macromolecule alternatively passing through crystalline and amorphous regions (Fig. 1) is now replaced by the folded chain crystal model with the majority of molecules folding back at the crystal surface. But still a few pass through the surface and enter the next crystal. Such connection of crystalline lamellae by tie molecules significantly contributes to the mechanical strength of polymer solids. The best example for such a structure are fibers with high longitudinal elastic modulus and strength as a consequence of the great many tie molecules connecting the well stacked crystalline lamellae oriented perpendicular to the fiber axis.

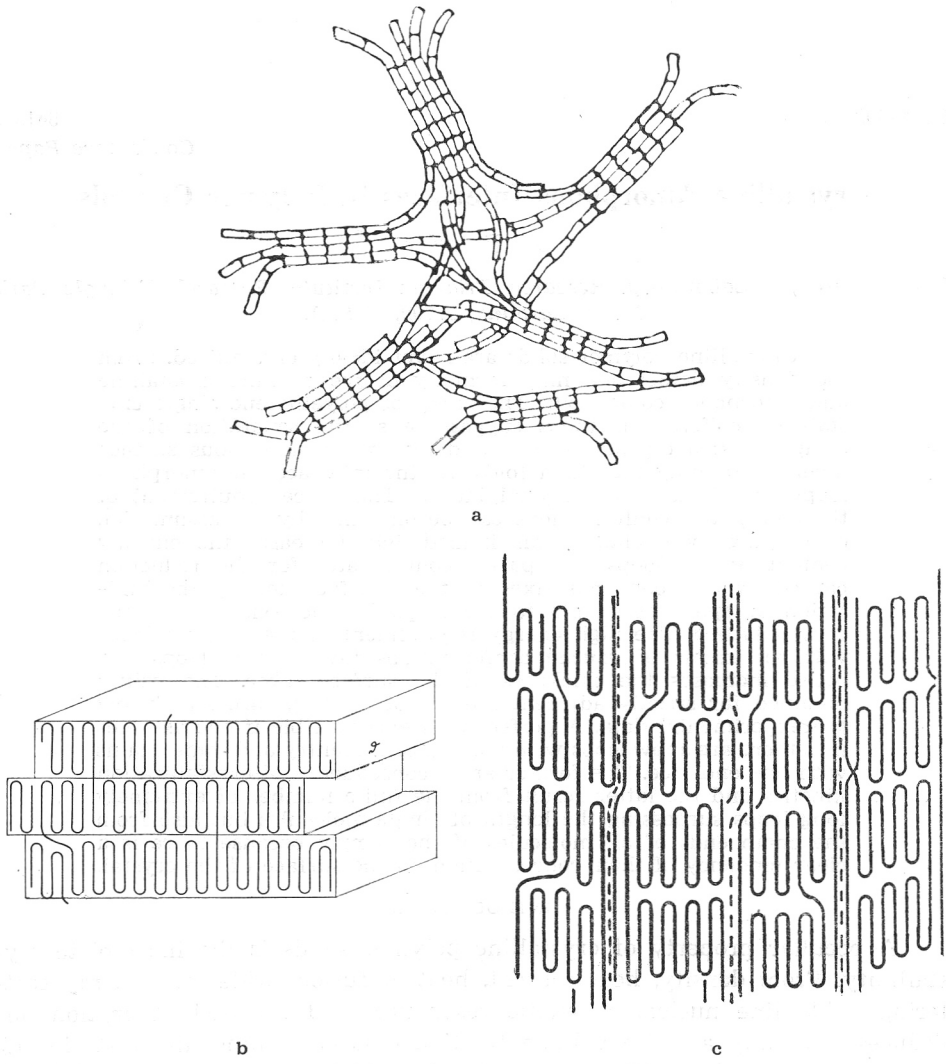

Fig. 1. Molecular models of crystalline polymer solid: (*a*) fringed micelles;[1] (*b*) folded chain crystals; (*c*) fiber structure. In the last two models the amorphous content is contained in defects inside the crystals and in the fold containing surface layers.

In the folded chain crystal model the amorphous component is located in crystal defects and in layers between adjacent crystal blocks. These layers contain chain folds, tie molecules and rejected noncrystallizable impurities. One sees that in such a layer there is an intimate connection between the crystalline substrate and the amorphous layer because the majority of chain sections in the latter are parts of molecules included in the former. The crystalline pattern at the interface hence influences the space available to single chain loops and tie molecules in the surface layer.

The conditions on the interface between the crystal core and the fold containing surface layer are of primary importance for the understanding

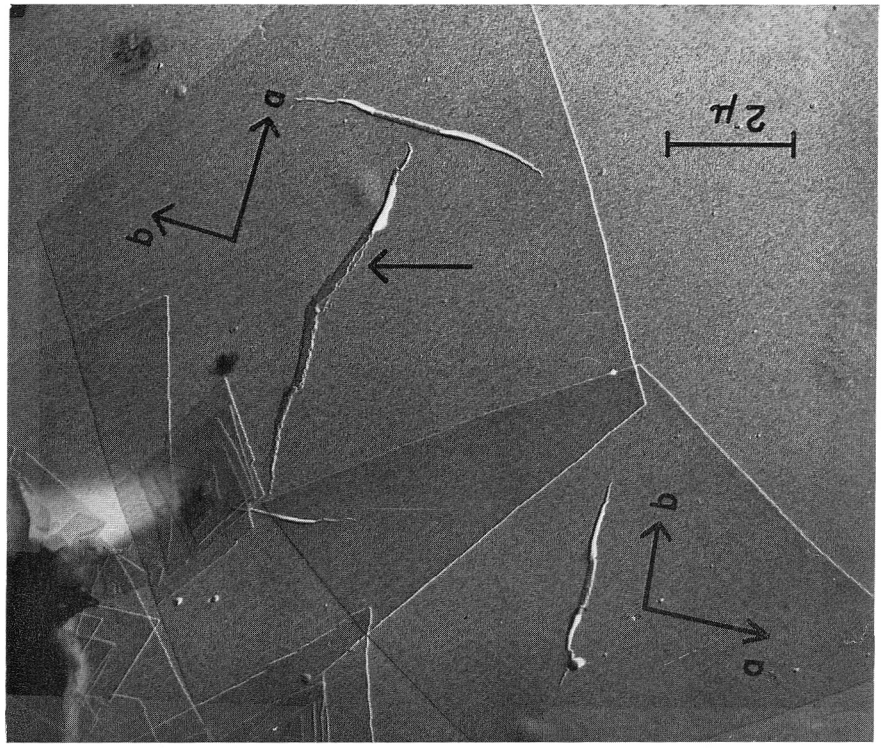

Fig. 2. Electron micrographs of (*a*) losenge type collapsed pyramids.

[To face page 336]

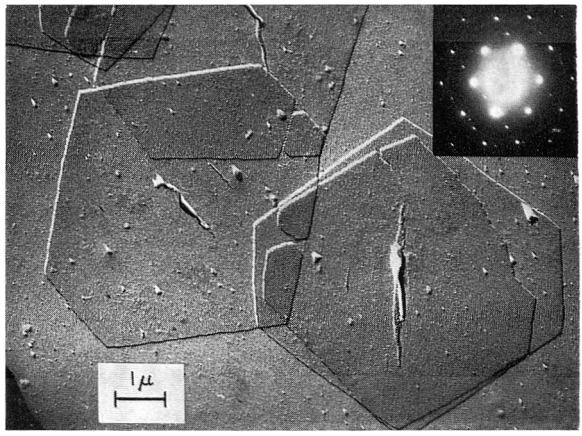

b

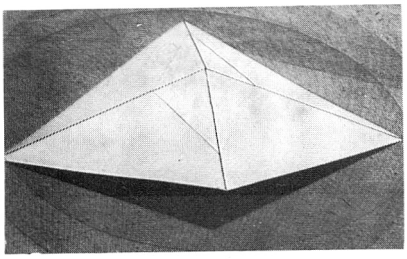

c

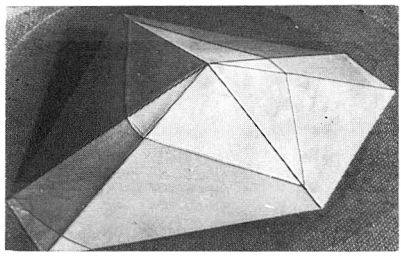

d

Fig. 2. Electron micrographs of (*b*) collapsed truncated pyramids; (*c*) model of four plane pyramid; (*d*) model of six plane pyramid. The flattened pyramids exhibit pleats caused by the collapse of the spatial structure. In the models the boundary of the upper pyramid is a (091) cross section.

[To face page 337]

of the solid state of crystalline polymers. The situation can be best studied with polymer single crystals where one has no unwanted complications by the supercrystalline organization of the bulk material (spherulites in the isotropic solid, stacks of lamellae in the fiber). The most studied system and also best understood is linear polyethylene.[2]

Amorphous Surface Layers of Polyethylene Single Crystals

Polyethylene single crystals obtained from dilute solutions are either four plane pyramids or truncated pyramids or ribbon-like lamellae (Fig. 2). As a rule the pyramids collapse during preparation for electron microscopy and assume a losenge type shape. The lateral dimensions may be up to a few micrometers. The thickness of the crystals, however, is very small between 100 and 200 Å dependent on temperature of formation. Since the polyethylene chains are nearly perpendicular to the surface and much longer than the crystal thickness L, *i. e.*, about 4500 Å for M = 50,000, they must fold back at the surface and re-enter the crystal lattice. The surface folds in the losenge type crystals are in the (110) crystal plane and contain each at least four maybe five CH_2 groups in *gauche* conformation. They do not fit the crystal lattice. Their space requirement seems to enforce the pyramidal shape of the at 20° C (Jackson, Flory and Chang,[5] Swan[10])

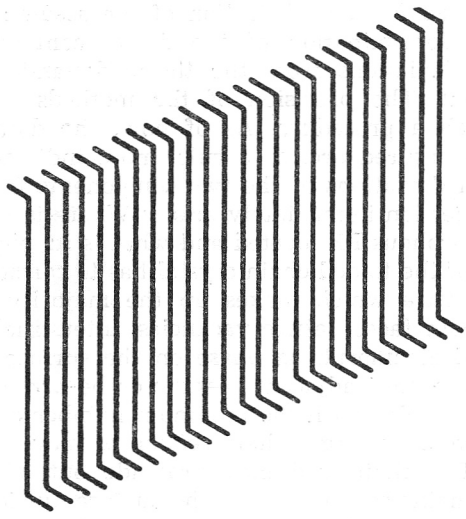

Fig. 3. The folds of the (110) plane are staggered as a consequence of their space requirement hence imposing a pyramidal instead of a planar growth habit.

The density of PE single crystals varies between 1.000 (Kawai and Keller[5]) and 0.96 g cm^{-3}. [6-9] The ideal crystal lattice density is $\varrho_c = 1.000$. The observed density defect of single crystals must be the consequence of isolated or concentrated crystal defects (vacancies). From a purely formal point of view, one can assign to such a crystal an ideal crystal fraction α with $\varrho_c = 1.000$ and an amorphous fraction $(1 - \alpha)$ with the density of supercooled melt $\varrho_a = 0.856$ at 20° C (Jackson, Flory and Chang,[5] Swan[10])

$$\varrho = \alpha\varrho_c + (1 - \alpha)\,\varrho_a \tag{1}$$

$$\alpha = (\varrho - \varrho_a)/(\varrho - \varrho_a) \tag{2}$$

The crystallinity of a single crystal is usually between 0.75 and 0.95.

The variation of α with crystallization conditions is very little understood. In some cases one certainly has crystals with a crystallographically perfect surface which permits a nearly perfect match of the crystalline lattice of two superimposed crystals so that the Moire pattern in dark-field electron microscopy disappears and one observes well-developed dislocation loops (Holland and Lindenmeyer[11]). With such crystals one suspects nearly 100% crystallinity, *i. e.*, a density close to ϱ_c. Most single crystals, however, have a smaller density $\varrho < \varrho_c$ and hence $\alpha < 1$.

There is a series of methods (specific heat, heat of fusion, wide-angle x-ray scattering, invariant of small angle x-ray scattering, infrared absorption wide line NMR) yielding pretty well agreeing information about the ratio between crystalline and amorphous component. All determinations are based on the extreme two-component model. The crystalline component is assumed to possess an ideal crystal lattice without defects and the amorphous one is just supercooled melt with random chain orientation. These assumptions are certainly exaggerated and one therefore expects disagreement among the data for crystallinity fraction α determined by the different methods. The deviations could, however, be used for a modification of the assumptions about the two states, *i. e.*, for the determination of the defect content of the crystalline component and the deviations from the thermodynamic equilibrium of the amorphous component. The precision of the methods, however, is not yet good enough for such a procedure. As of now, the data agree pretty well and the deviations measured are, as a rule, more indicative of the errors of measurement than of deviations of the two components from the ideal values.

The following question immediately arises: Where is the quite appreciable fraction $1 - \alpha$ of amorphous PE located and what is its physical state? A more detailed description of the folded chain crystal has to consider the unperturbed, *i. e.*, ideal, crystal lattice which makes up the majority of the crystal, the chain folds at the main faces, lattice vacancies, interstitials, and eventually a true, more or less ideal amorphous phase on the surface of the crystal. The chain folds may have either adjacent reentry or be arranged as on a switchboard. They may be regular with the minimum number of CH_2 groups needed for a fold or may contain a larger chain section or may represent mixtures of these possibilities. The chain end may protrude out of the fold-containing surface so that it remains somewhere on the surface outside the crystal lattice (cilia) and hence contributes to the »amorphous« phase at the crystal surface or it may be located within the crystal. In the latter case a point or a row lattice vacancy is created depending on to what extent the lattice points in the continuation of the chain under consideration are occupied by elements of other chains. Such a vacancy may give rise to an edge dislocation, *i. e.*, the insertion of a (h, k, 0) plane which can be easily observed in the Moire pattern of two superimposed single crystals.

Another type of concentrated crystal defect is connected with the mosaic structure. From the radial width of wide-angle x-ray reflections of single crystal mats, Hosemann *et al.*[12] conclude that the coherent crystal lattice in

a PE single crystal has lateral dimensions of about 300 Å. The boundary between slightly mismatched folded chain blocks is presumed to contain a planar arrangement of screw dislocations or kinkens.[13] The mosaic structure is also directly observable in the fine structure of the isointensity lines of the Moire pattern which are not smooth lines but show irregular fluctuations with an average period of a few 100 Å. It also is believed to play an important role in plastic deformation.[14] The boundary between the blocks deforms easier by chain slip and hence under applied stress proceeds rapidly to such an extent that the mechanical cohesion breaks down. The crystal fails preferentially along such a boundary. A crack forms which under favorable conditions may be bridged by microfibrils pulled out of the crystal and composed of folded chain blocks and of chains partially unfolded at the fracture plane during the process.

There are some experimental data which unambiguously favor the location of all or of the larger part of the amorphous component on the twofold containing surfaces of the single crystal.

If one anneals a single crystal mat in a temperature range sufficiently close to the melting point, one observes a linear increase of the long period, *i. e.*, of single crystal thickness, with the logarithm of annealing time. The

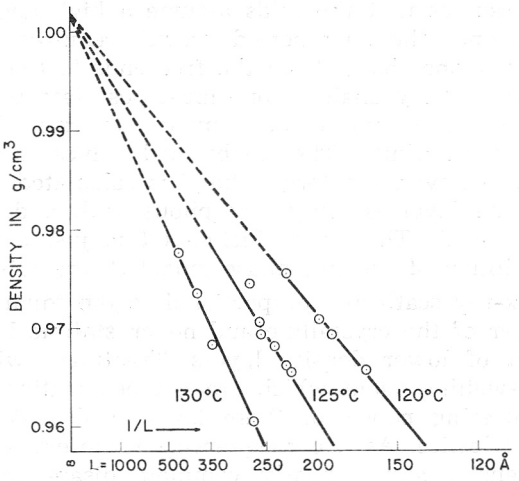

Fig. 4. Density of single crystal mats as a function of reciprocal thickness 1/L of lamellae.[6] The mats were annealed at 120, 125 and 130° C.

density of such a mat plotted against 1/L yields a strainght line[6] (Fig. 4) which can be represented by

$$\varrho = \varrho_c - A/L = \varrho_c - (\varrho_c - \varrho_a)\, l/L \tag{3}$$

The ordinate intercept ϱ_c is the ideal density of the crystal core. The constant A is a function of annealing temperature. It can be interpreted as a density defect associated with an amorphous layer of thickness l between superimposed crystals or as two amorphous layers of thickness $l/2$ each positioned at the fold-containing surfaces of the crystals (Fig. 5). The constant A and hence the thickness l incerease with the annealing temperature but are independent of

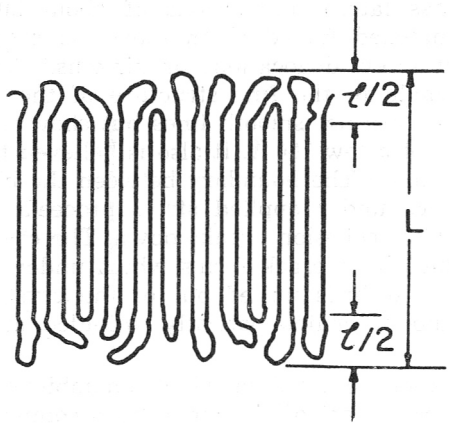

Fig. 5. The single crystal lamella with the thickness L, two amorphous layers of thickness $l/2$ each and the crystal core of thickness L—l.

lamella thickness L. The latter fact makes it unlikely that the density defect is spread over the whole interior of the crystal. A much simpler model is obtained if one assumes that the folds assume a high degree of irregularity during annealing since the long period growth requires a large amount of mass transport along the chains from the free ends to the folds at the center of the macromolecule.[15] By analogy, one must postulate that also unannealed crystals possess two such »amorphous« surface layers if their density shows a less that 100% crystallinity. The so-obtained values A or l are plotted in Fig. 6. One must, however, not forget that l is calculated on the basis of the assumption that the layer is truly amorphous with a density ϱ_a. The true experimental data is A. The layer thickness l is just a very useful if not an accurate description of the two-phase model of the single crystal.

Small angle x-ray scattering proportional to the square of the difference of scattering power of the crystalline and noncrystalline layers strongly supports the concept of lower density layers. Treatment with iodine or high electron density swelling agent which are not penetrating the crystal lattice increases the scattering power of these layers and may make it equal to the denser crystal lattice. As a consequence one observes a drastic decrease of scattering intensity and a nearly complete disappearance of scattering maxima corresponding to lamella thickness L[15a].

A particularly convincing support for the concept of amorphous surface layers is obtained from fuming nitric acid treatment data.[16] The weight loss first proceeds at a rather fast, constant rate which, after a while, changes to a smaller but again constant value. The inflection occurs at a time when the weight loss just corresponds to the amorphous content of the sample (Fig. 7). Concurrent measurements of molecular weight of the sample show first a very rapid drop from the initial viscosity average $M_v = 50{,}000$ to a value which corresponds to the thickness of the crystalline core $L - l$ and then a slower decrease in pace with the weight loss, *i. e.*, with the acid attack which makes the crystal thinner and thinner. The experimental data are best represented by the assumption that the acid first attacks the chains in amorphous conformation at the crystal surface, breaks the folds, and rapidly

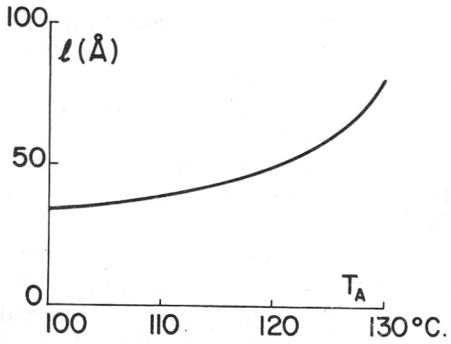

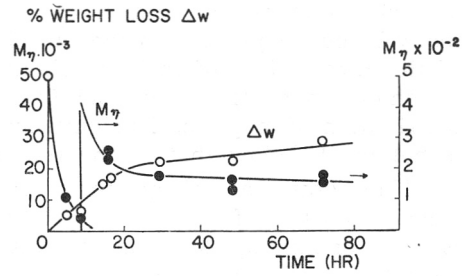

Fig. 6. Twice the surface layer thickness l as function of temperature of annealing.[6]
Fig. 7. Weight loss in % and viscosity average molecular weight as a function of exposure of annealed polyethylene single crystals to fuming nitric acid.[16]

destroys the remaining free ends in the amorphous layer. The attack is slowed down as soon as the amorphous component is completely removed so that all remaining chains are in crystalline conformation.

Theory of the Amorphous Surface Layer

The high concentration of crystal defects in the fold-containing surface layers, which may be considered as amorphous, certainly needs some theoretical justification. Flory[14] assumes that the reentry of the chain is at random (switchboard model) and thus automatically obtains an amorphous surface layer. Fischer[18] calculates the free energy of an amorphous loop with a distance r between the points where the loop is attached to the crystal lattice and obtains a surface layer with a finite thickness (loop length) increasing with temperature and r. His model is closely related to the switchboard model but with identical loops. To obtain reasonable agreement with experimental data (Fig. 4), he must assume a value r of about 30 Å, which is very nearly 6 times the distance between loop ends for adjacent reentry in the (110) plane. The calculated l, however, does not increase with increasing temperature as rapidly as the experimental values. In addition, one is faced with the problem of how to find space for the amorphous conformation of the densely packed loops which require nearly twice as large a cross section for every chain as in the crystal lattice.

If, however, one assumes that the loop length is random, one solves the problem of space and entropy[2,10] (Fig. 8). The existence of short and long

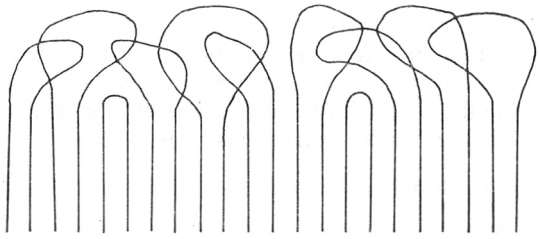

Fig. 8. Model of amorphous surface layer with irregular loops and adjacent reentry.

loops creates enough room in sufficient distance from the crystal core to permit the chain to assume a more or less random conformation. The surface layer is hence composed of some very short, even perfectly regular loops and of many longer loops with amorphous chains. As a consequence, the outer surface of the crystal, *i. e.*, of the amorphous surface layer has a surface free energy which does not differ very much from that of a supercooled liquid. The random distribution of loop lengths significantly increases the entropy which therefore is not much below that of the relaxed liquid.

The additional entropy term favors the formation of longer loops in the same way as the formation of Schottky defects in a crystal is favored by the entropy of mixing. So, owing to this term, a broad melting range is obtained even for small end-to-end distances of the loops. Moreover, the formation of longer loops is favored by the fact that short loops have a larger fraction of *gauche* conformations than a chain in the melt.

On the basis of statistical mechanics, Zachmann and Peterlin[19] obtain for the loop length distribution, *i. e.*, for the number ν_N of loops with N statistically independent chain elements

$$\nu_N/\nu = \frac{\exp\left[-\Delta F_l\,(N)/kT\right]}{\Sigma \exp\left[-\Delta F_l\,(N)/kT\right]} \tag{4}$$

where ν is the total number of loops, $\Delta F_l\,(N)$ the change in free energy occurring when U units of the crystal are transformed to a loop, k is Boltzmann constant and T is absolute temperature. The average loop length turns out to be

$$< N > = \frac{\Sigma N \nu_N}{\nu} = \frac{\Sigma N \exp\left[-\Delta F_l\,(N)/kT\right]}{\Sigma \exp\left[-\Delta F_l\,(N)/kT\right]} \tag{5}$$

In all these formulae the summation index N goes from N_1, the number of units in the shortest loop possible to infinity.

In order to evaluate Eqs. 4 and 5 one needs an expression for $\Delta F_l\,(N)$. Let us consider first the enthalpy contribution $\Delta H_l\,(N)$ to this quantity. The enthalpy of a unit in a loop will be the same as that in the melt except that in comparatively short loops there occurs a larger fraction of *gauche* conformations than in the melt. The additional enthalpy caused by this effect depends on the length of the loop N and is denoted by $\sigma_g\,(N)$. For larger N, $\sigma_g\,(N)$ will be zero. With the help of this function, one can write

$$\Delta H_l\,(N) = N\,\Delta \bar{H}^0 + \sigma_g\,(N) \tag{6}$$

where $\Delta\bar{H}^0$ is the melting enthalpy per monomer unit.

The evaluation of the entropy contributions $\Delta S_l\,(N)$ is more complicated. The entropy of the units in a loop is not the same as in the melt, because the ends of the loop are fixed and the volume available to it is limited by the presence of the crystals. This limitation is extremely important and strongly affects the results. Under these conditions, one obtains:

$$\Delta S_l\,(N) = N\,\Delta \bar{S}^0 + k \ln\left[f_p^*\,(N, h)\,P\,(N, h)/f_p\,(N)\right] - k \ln 6 \tag{7}$$

In this formula P (N, h) is the probability that one end of an isolated chain lies a distance h from the other chain end, within a volume with the dimen-

sions of the chain element. If the limitation of space by the crystal is taken into account, this probability is given by

$$P(N, h) = [3/2\,\pi\,(N-1)]^{3/2}\,\{\exp[-3\,h^2/2\,(N-1)] - \exp[-3\,(h^2+4)/2\,(N-1)]\} \quad (8)$$

The quantities $f_p^*(N, h)$ and $f_p(N)$ in Eq. 7 are packing factors for the non-crystalline region and the melt, respectively. They make allowance for the decrease in the number of available conformations of a chain caused by the presence of the other chains. One hence obtains for the free energy difference

$$\Delta F_l(N) = \Delta H_l(N) - T\,\Delta S_l(N) = N\,\Delta\overline{H}^{\circ}\,(T^{\circ}_m - T)/T^{\circ}_m + \sigma_g(N) +$$

$$kT \ln [f_p^*(N, h)\,P(N, h)/f_p(N)] + k \ln 6 \quad (9)$$

This value has to be inserted in Eqs. 4 and 5.

In order to evaluate the expressions for ΔF, ν_N and $<N>$ one has to choose appropriate values for the independent chain element, the distance h, the energy parameter σ_g and the packing factor f_p^*. The number of CH_2 groups corresponding to a model chain element has to be chosen in such a way that the entropy of melting is the same for the model chain as for the real molecule. The configurational contribution to the entropy of melting for the model chain is 0.82 k/chain unit. The polyethylene chain has a melting enthalpy of 940 cal/mol CH_2, a melting point of about 415° K and, from this, a melting entropy of 2.3 cal/degree mol CH_2 which corresponds to 1.15 k/CH_2. This value gives not only the configurational contribution to the entropy but also other contributions, the exact amount of which is not known. Considering this, a correspondence of the unit of the model chain to one CH_2-group seems to be quite reasonable and hence was assumed in the actual calculations.

In polyethylene, loops can go among others either in the (110) direction or in the (100) direction. In the first case the end-to-end distance h for adjacent reentry is 4.05 Å; that corresponds to nearly three times the C—C distance. The shortest possible loop is formed by a completely rigid arrangement of 4 or 5 CH_2-groups in *gauche* conformation. This situation is quite reasonably approached in our model if one assumes an end-to-end distance of three units. In that case the shortest possible loop is formed by four rigidly arranged units (see Fig. 9). In the second case, for loops in (100) direction,

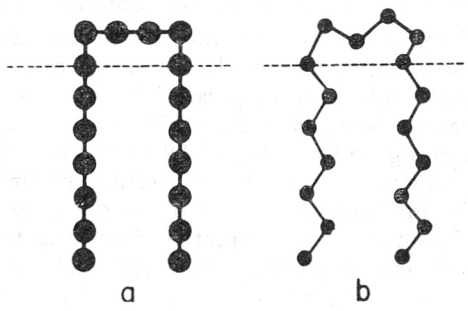

Fig. 9. Schematic representation of the shortest possible loop in case of adjacent reentry (*a*) for the model chain and (*b*) for the real polyethylene chain.

the end-to-end distance in polyethylene is 8.4 Å, which means five C—C distances, *i. e.,* five units.

The additional enthalpy $\sigma_g(N)$ is caused by the increased numbers of *gauche* conformations in the loops. In polyethylene, the shortest loop possible gives rise to an additional surface energy of 60 erg/cm² corresponding to 3180 cal per mole loops. In our model the same value is attributed to the shortest loop with $N_1 = 4$ or 5 corresponding to a (110) or (100) loop, respectively. For larger N we first assumed $\sigma_g(N)$ to be zero. This, of course, is not completely correct. Therefore, we also considered the case that $\sigma_g(N)$ decreases linearly with increasing N up to $N = 9$ where it vanishes and remains zero for larger N. The extreme case that all $\sigma_g(N)$ vanish including that for $N = 4$ was included for comparison.

The packing factor was obtained by a derivation following closely that given by DiMarzio.[20] The main difference is caused by the fact that DiMarzio considers chains with one end fixed at the crystal-amorphous interface and the other end free whereas in our case both ends are fixed at the interface. One obtains

$$\ln f_d^*(N, h) = N(1 - \alpha_1) \ln(1 - \alpha_1) + 2N(1 - \alpha_2) \ln(1 - \alpha_2)$$

with

$$\alpha_1 = -1/3 + (2/3)[1 + 3h^2/(N+1)^2]^{1/2}$$

$$\alpha_2 = (1 - \alpha_1)/2$$

It turns out that modifications of f_p^* and even its replacement by the value in melt

$$\ln f_p(N) = -N \ln 2.25$$

hardly affects the distribution and average value of loop lengths.

The remaining two quantities, the melting point and the enthalpy of melting, were assumed to be, in accordance with the values of polyethylene, 415° K and 940 cal/deg mole CH_2.

The details of calculation are described in the already quoted paper by Zachmann and Peterlin.[10] Here only the main results will be reported. Special attention was given to the actual loop length distribution and the average value yielding the thickness of the amorphous surface layer as function of temperature and the distance h of the ends. The influence of free ends was not yet considered.

If one puts $\sigma_g = 0$ for all $N > N_1$ one obtains $< N >$ as function of supercooling $T_m^o - T$ for values of the end-to-end distance h as shown in Fig. 10. Let us consider for example the results for $h = 4$ corresponding to adjacent reentry. At large supercooling, a loop consists of $< N > = 8$ units on the average. With increasing temperatures, $< N >$ increases to reach a value of 18 at 10° C supercooling and a value of 39 at the metlting point. From this, it is seen that a considerable amount of melting occurs below the melting point. But even at the melting point the loop length does not become infinite; that is, the crystal does not melt completely from the top surface. For comparison, in Fig. 10 the experimentally observed melting behavior calculated from data of Fischer and Schmidt[6] is shown as a dotted curve. It can be seen that for adjacent reentry the experimental and theoretical values differ appreciably. But if an end-to-end distance of about $h = 10$ corresponding to $r = 15$ Å

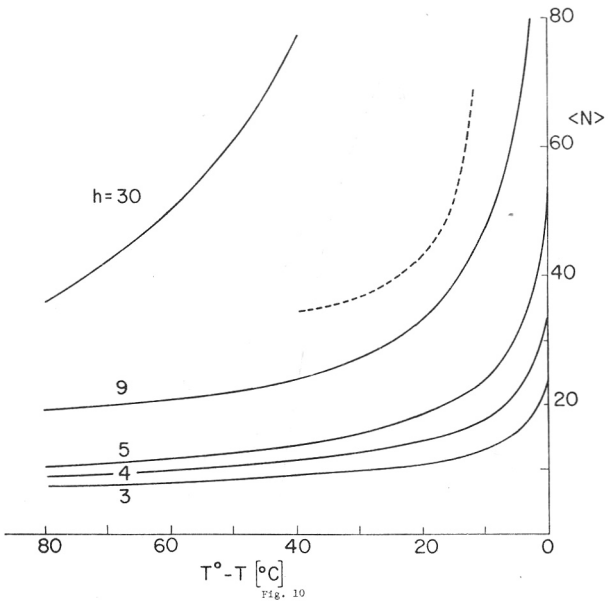

Fig. 10

Fig. 10. Average loop length $\langle N \rangle = l/1.5$ Å as function of supercooling, $T_m^0 - T$, for different end-to-end distances h of the loops if $\sigma_g (N > 4) = 0$.[18] The experimental curve (dotted line) represents the values from Fig. 6.

is assumed, good agreement is obtained. With identical loops, however, Fischer[15] needs a distance of 30 Å for agreement with experimental data.

Fig. 11 gives the loop lengths distribution function ν_N/ν obtained in the case $h = 3$, at the melting point and at supercooling $\Delta T = 40^0$ C. One sees that there occurs a sharp maximum for loops of about 5 units at both temperatures. The increase of average loop length with increasing temperature is due to an increase of the number of loops composed of more than 12 units. The contribution of longer loops is particularly conspicuous very close to the melting. But still in the temperature range up to 3^0 C below the melting point, even for an end-to-end distance of $h = 30$ the main contribution to melting arises from loops with less than 300 units.

Some studies were also performed concerning the sensitivity of the results to the choice of the values of the parameters available. Fig. 12 shows the influence of the function $\sigma_g (N)$ which takes into account the increased number of *gauche* conformations in the loops. Curve a was obtained under the assumption that all $\sigma_g (N)$ are zero. In curve b, the $\sigma_g (4)$ was $2.16 \cdot 10^{-13}$ erg/fold corresponding to 3180 cal/mole folds, and all other $\sigma_g (N)$ were equal to zero, just as in Fig. 10. For curve c it was assumed that $\sigma_g (4)$ has the same value as for curve b, but that $\sigma_g (N)$ decreases linearly from that value to zero in the range from $N = 4$ to $N = 9$. As expected, one finds increasing melting with increasing values for $\sigma_g (N)$. In the last case (c) the thickness of the surface layer is about 30% larger than in the case (b) represented in Fig. 10 and hence is a little closer to the experimental value of Fischer and Schmidt althougt the fit is far from satisfactory.

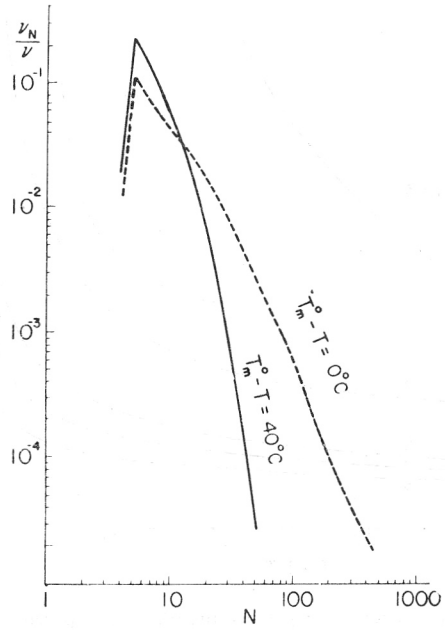

Fig. 11. Loop length distribution for adjacent reentry (h = 3) at the melting point (broken line) and at 40° C below it (full line) under the assumption σ_g (N > 4) = 0.[18]

In a further calculation, the entropy of the noncrystalline sheet formed by the loops was determined and the results are shown in Fig. 13. Plotted is the difference between the entropy of the melt S_m and the entropy of the noncrystalline layer S, both per monomer unit, as a function of supercooling.

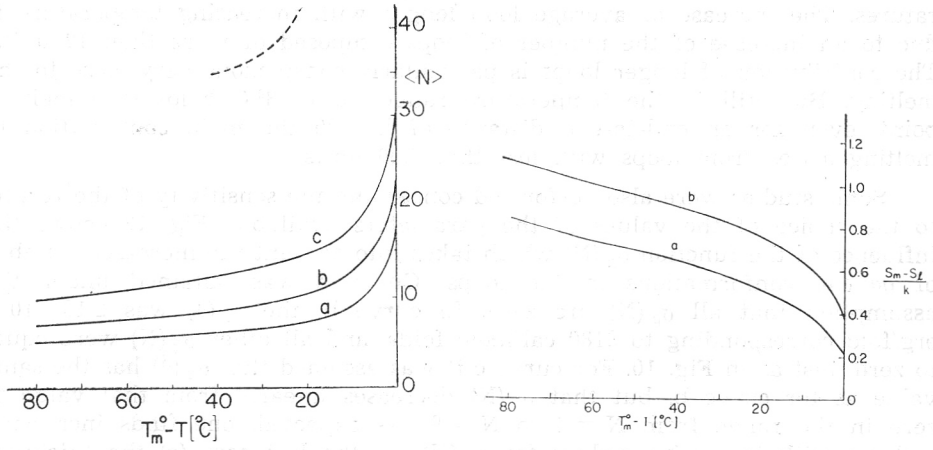

Fig. 12. Influence of the function σ_g (N) on the calculated average loop length <N> for h = 3. (*a*) σ_g (N) = 0 for N $\geqslant$ 4; (*b*) σ_g (N) = 0 for N $\geqslant$ 5: (*c*) σ_g (N) drops linearly to zero from N = 4 to N = 9.[18] The broken line represents the experimental values from Fig. 6.

Fig. 13. Difference between the configurational entropy of the melt and that of the loops per segment (*a*) with random length loops and (*b*) with identical loops.[18]

Curve b was obtained without, and curve a was obtained with the mixing term $k\Sigma \ln (\nu_N/\nu)$. One sees that even with the mixing term the entropy of the noncrystalline sheet is lower than that of an equivalent melt. This is true also for the case where all $\sigma_g(N)$ are zero. Therefore, the free energy of the crystal plus surface layer is larger than that of an ideal crystal formed by the same amount of the material without any loops, but it is lower than that of a crystal with ideal folds, that is, with shortest possible loops. That means that as far as the melting behavior and particularly the depression of the melting point is concerned the surface free energy is a little less than in the case of sharp loops in excellent agreement with calorimetric data. Moreover, it supports the estimate of maximum thickness of surface layer by Peterlin[2] based on the assumption that the free energy of the ideal liquid layer and liquid-air surface energy together equals that of the crystal with sharp loops and hence high surface energy.

In principle, the change in average loop length, is reversible with temperature. But it needs a readjustment of loop length distribution which can be only achieved by pulling the chains through the crystal core so that the length of the loops is individually increased or decreased. At lower temperatures, however, the diffusion of the chain through the crystalline lattice may become so slow that the equilibrium loop length distribution cannot be reached within finite times. At these temperatures, during cooling of the sample, some crystallization can still occur without any diffusion of the chains. But the presence of shortest loops makes the crystallization of longer loops nearly impossible without either chain diffusion through the crystal lattice or formation of large crystal lattice defects and additional surfaces. Hence the amount of molten material, in this case, is given by the loop length distribution existing when the diffusion of the chain is frozen in. But it also depends on the maximum temperature of the heat treatment because it determines the maximum amount of amorphous material and hence the amount of chain diffusion through the crystal lattice needed for readjustment during cooling. The larger this amount the earlier the slowness of diffusion will freeze in the loop length distribution. As a consequence, one observes at room temperature a surface layer thickness dependent on the temperature of annealing (Fig. 6).

At temperature where diffusion of the chains in the crystal lattice takes place, there occurs another effect worth mentioning. It can be seen from Fig. 9 that the lengths of some loops approach the length of an entire molecule. In most polyethylene samples the number average molecular weight is about 5000 to 6000 corresponding to 400 chain elements. In the process of forming such loops, it may happen that one end of the molecule diffuses out of the crystal after which the chain no longer belongs to the system of loops considered in the theory. So there is a tendency for the formation of chains with one end free (cilia). In turns out that in thermal equilibrium the cilia are much longer than loops and hence yield thicker surface layers.

From Fig. 13 one sees that the experimentally observed surface layer thickness is still appreciably larger than the calculated one even if one considers the higher energy content of the shortest loops. The discrepancy becomes larger if one takes into account that one measures at room temperature not the equilibrium thickness of the surface layers corresponding to the highest temperature of the preceding thermal treatment (annealing

temperature) but only the irreversible part of it which remained frozen in during cooling to room temperature as a consequence of the too rapidly decreased chain mobility through the crystal lattice. That means that the experimental $< N >$ is larger than plotted in Fig. 13 and hence still larger the difference between $< N >_{exp}$ and $< N >_{theor}$.

A better fit may be achieved by dropping the requirement that all loops have adjacent reentry. The crystallization kinetics certainly does not exclude some loops with more or less random reentry occurring in the case that the same macromolecule starts crystallizing at two separated sections of the growing crystal. The intermediate section will be prevented from complete inclusion in the crystal lattice and will hence form a loop with larger than minimum distance between the fixed ends.

On the other hand, one derived a final probability for cilia formation caused by the fact that some loops are becoming larger than full length of the molecules of the sample. Moreover, one knows that molecular ends tend to be on the crystal surface[21] thus producing cilia even in absence of a surface layer with loose loops. Therefore one has to consider also the contribution of cilia to the surface layer. As already mentioned the molecules with one end fixed and the other one free have a higher entropy than loops and hence at equal supercooling produce a thicker amorphous layer. Mixed with loops they increase the value N obtained for loops alone and hence bring the calculated value closer to the experimental data. Moreover, the rapid increase of the cilia fraction with approaching the melting point and their higher entropy are yielding so large a limiting thickness of the surface layer that a complete surface melting of the folded chain crystal becomes a real possibility. A detailed consideration of this case will be completed soon.

CONCLUSIONS

Sufficient experimental evidence is accumulated for the existence of a crystal-amorphous interface at the fold containing surface of polymer crystals. The crystal lattice fixes the ends of the loops in the amorphous layer. In order to accommodate the amorphous chain conformations requiring more space than crystallized chains one has to assume irregular loops with widely varying length. This immediately increases the entropy and decreases the free energy of the amorphous layer. On the other hand, the inaccessibility of space occupied by the crystal drastically reduces the entropy of the loops. A further effect is the concentration of high energy *gauche* conformations in the shortest sharp loops thus raising the enthalpy content above that of the free melt. A longer loop does not more need such an excess of *gauche* conformations and hence lowers the free energy per chain element. As a consequence large loops are favored thus producing a finite amorphous surface layer. Even with strictly adjacent reentry one obtains in thermal equilibrium a temperature dependence of surface layer thickness which is still substantially below the experimental data but has the proper dependence on supercooling. A small fraction of loops with random reentry and of cilia with one end free is needed for a fit between theory and experiment. With approaching the melting point the average length of the loops remains finite thus precluding a complete surface melting of single crystals. But such a possibility exists *via* rapidly increased fraction of cilia with increasing temperature.

REFERENCES

1. K. Hermann, O. Gerngross, and W. Abitz, *Z. Phys. Chem.* **B10** (1930). 2371. K. Hermann and O. Gerngross, *Kautschuk* **8** (1932) 181.
2. A. Peterlin, *J. Macromol. Sci.* (Phys.) **B3** (1969) 19.
3. O. H. Reneker and P. H. Geil, *J. Appl. Phys.* **31** (1960) 1916.
4. P. Ingram and A. Peterlin, *Encyclopedia of Polymer Sci. & Tech.*, Vol. 5, J. Wiley & Sons, New York, 1968, p. 204.
5. T. Kawai and A. Keller, *Phil. Mag.* **8** (1963) 91, 1973.
6. E. W. Fischer and G. F. Schmidt, *Angew. Chem.* **74** (1962) 551.
7. E. W. Fischer and R. Lorentz, *Kolloid-Z. & Z. Polymere* **189** (1963) 97; E. W. Fischer and G. Hinrichsen, *Polymer* **7** (1966). 195.
8. J. B. Jackson, P. J. Flory, and R. Chiang, *Trans. Faraday Soc.* **59** (1963) 1909.
9. G. M. Martin and E. Passaglia, *J. Res. Natl. Bur. Std.* **10A** (1966) 221.
10. P. R. Swan, *J. Polymer Sci.* **42** (1960) 525.
11. V. F. Holland and P. H. Lindenmeyer, *J. Appl. Phys* **36** (1965) 3049.
12. R. Hosemann, H. Čačković, and W. Wilkes, *Naturwiss.* **54** (1967) 278.
13. W. Pechhold, S. Blasenbrey, and S. Woerner, *Kolloid-Z. & Z. Polymere* **189** (1959) 14.
14. A. Peterlin, *J. Polymer Sci.* **C9** (1965) 61; A. Peterlin, P. Ingram, and H. Kiho, *Makromol. Chem.* **86** (1965) 294.
15. A. Peterlin, *J. Polymer Sci.* **B1** (1963) 279; *Polymer* **6** (1965) 25.

15a. V. A. Marikhin, A. J. Slutsker, and A. A. Yastrebinskii, *Fiz. Tverd. Tela* **7** (1965) 441.

16. A. Peterlin and G. Meinel, *J. Polymer Sci.* **B3** (1965) 1059; A. Peterlin, G. Meinel, and H. Olf, *J. Polymer Sci.* **B4** (1966) 399; D. J. Blundell, A. Keller, and T. Connor, *J. Polymer Sci.* (A-2) 5 (1967) 991.
17. P. J. Flory, *J. Am. Chem. Soc.* **84** (1962) 2857.
18. E. W. Fischer, *Kolloid-Z. & Z. Polymere* **218** (1967). 97.
19. H. G. Zachmann and A. Peterlin, *J. Macromol. Sci.* (Phys.) **B3** (1969) 495.
20. E. A. DiMarzio, *J. Chem. Phys.* **36** (1962) 1563.
21. A. Keller and D. J. Priest, *J. Macromol. Sci.* (Phys.) **B2** (1968) 479.

IZVOD

Granica faza kristalno/amorfno u polimernim kristalima

A. Peterlin

Kristalizacija u čvrstim polimerima nije nikad idealna. Udjele kristalne i amorfne faze moguće je odrediti mjerenjem defekata u gustoći. Razne metode proučavanja sugeriraju model kristalne jezgre i dvaju površinskih slojeva koji sadrže povijene lance. Prostorni raspored amorfne konformacije može se protumačiti samo pretpostavkom o različitoj dužini petlji. Posljedica toga je povećavanje entropije petlji i djelomična kompenzacija za gubitak entropije uslijed toga, što su krajevi petlji fiksirani na površini, kao i jer je prostor raspoloživ petljama ograničen postojanjem kristalne strukture. Visoki sadržaj energije najkraćih petlji, i to onih sa suviškom *gauche* konformacije, favorizira stvaranje dugih petlji, te time povećanje debljine površinskog sloja. Vrijednosti proračunate za striktno najuže vraćanje svih petlji još su uvijek ispod eksperimentalnih podataka. Čini se, da je potpuno slaganje proračuna moguće ako se pretpostavi postojanje petlji s širim vraćanjem, i lanaca s jednim slobodnim krajem. Prvi su uvjetovani kinetikom kristalizacije, a drugi su ili rezultat konačnog broja ekstremno dugačkih petlji, koje prelaze dužinu pojedinih molekula, ili kraja lanaca molekula u uzorku koji imaju tendenciju koncentriranja na površini kristala.

CAMILLE DREYFUS LABORATORY
RESEARCH TRIANGLE PARK, N. C. USA